

## **VIII- II -1. Project Research**

### **Project 2**

Y. Ohkubo

Research Reactor Institute, Kyoto University

### Objective and Participating Research Subjects

The main objectives of this project research are the investigation of the nuclear structure of unstable neutron-rich nuclei and also the local properties of materials using short-lived nuclei.

This period is the third and last year of the project.

The research subjects (PRS) executed in this period are as follows:

- PRS-1 Technique of transferring radioactive atomic nuclei implanted in dry ice film
- PRS-2 Identification of the excited levels of  $^{156}\text{Pm}$  through the decay of  $^{156}\text{Nd}$
- PRS-3 Decay scheme of  $^{150}\text{Ce}$
- PRS-4 (a) Extranuclear dynamic motion around  $^{111}\text{Cd}(\leftarrow^{111}\text{Ag})$  doped in AgI nanoparticles; (b) TDPAC measurements of hyperfine fields at Pm impurities in Fe
- PRS-5 Atmosphere dependence of local fields in Al-doped ZnO
- PRS-6  $^{197}\text{Au}$  Mössbauer study of Au nanoparticles
- PRS-7 Determination of the structure and electronic state of thiolate-protected hetero-metal cluster,  $\text{Au}_{24}\text{Pd}_1(\text{SC}_{12}\text{H}_{25})_{18}$ , by means of  $^{197}\text{Au}$  Mössbauer spectroscopy
- PRS-8 Characterization of Au in nickel oxide by  $^{197}\text{Au}$  Mössbauer spectroscopy

### Main Results and Contents of This Report

As a means to measure the charge distribution of an unstable nucleus, it is promising to make a muonic atom composed of the nucleus that are trapped in deuterium film and then to measure the energies of X-ray emitted from the muonic atom. However, it is unavoidable to deal with high radioactivity. One of the technical problems is how efficiently and safely long-lived radioactivity in the apparatus is removed after such an experiment is done. A. Taniguchi *et al.* (PRS-1) attacked this problem using a radioactive beam from KUR-ISOL and an apparatus designed for the present work and obtained good positive results.

M. Shibata *et al.* (PRS-2) investigated the level structure of the doubly-odd unstable  $^{156}\text{Pm}$  nucleus, a fission product of  $^{235}\text{U}$  + thermal neutron, at KUR-ISOL using a beam of  $^{156}\text{Nd}$  leading to excited levels of  $^{156}\text{Pm}$  and a clover detector consisting of 4 Ge crystals both in singles and add-back modes. They identified new excited levels of  $^{156}\text{Pm}$  and also new  $\gamma$ -rays accompanying the  $\beta^-$  decay of  $^{156}\text{Nd}$ .

At KUR-ISOL, Y. Kojima *et al.* (PRS-3) studied the decay scheme of unstable  $^{150}\text{Ce}$  for which quite insufficient information had been available, using a beam of  $^{150}\text{Ce}$  and measuring  $\gamma$ -ray singles and  $\gamma$ - $\gamma$  coincidences with two Ge detectors. They determined the half-life  $T_{1/2}$  of the ground state of  $^{150}\text{Ce}$  to be 6.05(7) s and identified new excited levels of  $^{150}\text{Pr}$  arising from the  $\beta^-$  decay of  $^{150}\text{Ce}$ .

Using the excited level with a nuclear spin  $I = 5/2$  and  $T_{1/2} = 85$  ns of  $^{111}\text{Cd}$  arising from  $^{111}\text{Ag}$ , W. Sato *et al.* (PRS-4a) observed dynamic perturbation patterns in the TDPAC spectra both at 453 and 333 K for AgI nanoparticles coated with a polymer (PVP), implying a hopping motion of Ag in AgI even below the  $\alpha$ - $\beta/\gamma$  phase transition temperature of 420 K for AgI with no polymer coating. Using an excited level with  $I = 5/2$  and  $T_{1/2} = 2.5$  ns of  $^{147}\text{Pm}$  arising from  $^{147}\text{Nd}$ , produced at KUR-ISOL, M. Tsuneyama *et al.* (PRS-4b) attempted to derive the magnetic hyperfine field at Pm implanted in ferromagnetic Fe foil by taking TDPAC spectra at room temperature, but could not reach meaningful results.

In order to see whether oxygen vacancies are formed in high-temperature vacuum, S. Komatsuda *et al.* (PRS-5) prepared two identical samples of 100 ppm Al-doped ZnO, annealed both in vacuum at 1273 K for a long time, and incorporated radioactive  $^{111\text{m}}\text{Cd}$  in one sample in air and in the other sample in vacuum both at 1373 K for 45 min. They took room-temperature  $^{111}\text{Cd}$ -TDPAC spectra for the two samples and obtained the results indicating that oxygen vacancies are formed in the sample annealed in vacuum while introducing  $^{111\text{m}}\text{Cd}$ .

Y. Kobayashi *et al.* (PRS-6) took  $^{197}\text{Au}$ -Mössbauer spectra at 13 K for two nanoparticles,  $\text{Au}_{25}(\text{SC}_{12}\text{H}_{25})_{18}$  and  $\text{Au}_{38}(\text{SC}_{12}\text{H}_{25})_{24}$  using  $^{197}\text{Pt}$  in Pt foil as a  $\gamma$ -ray (77.3 keV) source that was prepared by the (n,  $\gamma$ ) reaction at KUR and obtained the results that both spectra consist mainly of three Au components, the recoilless fractions of the corresponding components being different.

N. Kojima *et al.* (PRS-7) took  $^{197}\text{Au}$ -Mössbauer spectra at 16 K for two nanoparticles  $\text{Au}_{25}(\text{SC}_{12}\text{H}_{25})_{18}$  and  $\text{Au}_{24}\text{Pd}(\text{SC}_{12}\text{H}_{25})_{18}$  and obtained the results that Pd in the latter nanoparticle occupies the center of the Au core by comparing the two Mössbauer spectra.

Applying  $^{197}\text{Au}$ -Mössbauer spectroscopy at 8–15 K and X-ray absorption near edge structure to a study on gold nanoparticles supported on nickel oxide with three Au/Ni ratios, T. Yokoyama *et al.* (PRS-8) confirmed that two oxidation states of Au exist in each sample, Au(0) and Au(III), and also obtained the unexpected results that even with no specific reducing reagent Au(III) were reduced to Au(0).

## PR2-1 Technique of Transferring Radioactive Atomic Nuclei Implanted in Dry Ice Film

A. Taniguchi, P. Strasser<sup>1</sup>, M. Tanigaki and Y. Ohkubo

Research Reactor Institute, Kyoto University

<sup>1</sup>Muon Science Laboratory, IMSS, KEK

**INTRODUCTION:** The nuclear charge distribution is a fundamental property of atomic nuclei, for stable nuclei which has been investigated by various kinds of experimental methods [1]. However, little progress has been made for unstable nuclei mainly because a large amount of radioactivity is needed. Therefore, R&D for more efficient systems is being promoted.

Observation of the emitted X-rays from muonic atoms is one of the most effective methods for the investigation. The muon is in the same family as the electron, thus a negative muon ( $\mu^-$ ) can be captured in a Bohr orbit of a nucleus just as an electron and then a muonic atom is formed. Because a muon is 207 times as heavy as an electron, its lower orbits are close to the nucleus and the energies of the states depend sensitively on the nuclear charge distribution. By means of the muonic X-ray spectroscopy, therefore, information on the nuclear charge distribution can be obtained.

Recently, a new method using solid hydrogen film has been developed to produce radioactive muonic atoms. In this method, negative muons are injected to solid deuterium (D) film in which nuclei of interest (A) are implanted beforehand, thereby muonic atoms being formed through the highly-efficient muon transfer reaction:  $\mu^-D + A \rightarrow D + \mu^-A$ . The feasibility of this method was demonstrated using stable isotopes at the RIKEN-RAL muon facility and promising results were obtained [2]. However, several problems have to be solved before this method is applied to experiments for unstable nuclei. In this study, one such problem, concerned with handling of residual radioactivities in deuterium film after experiments, was attacked experimentally using a radioactive-isotope beam (RI beam) from KUR-ISOL and dry ice film.

**EXPERIMENTS:** In a preliminary experiment, it was established that dry ice film was formed on the surface of a copper block cooled with liquid N<sub>2</sub> (LN<sub>2</sub>) flow by spraying CO<sub>2</sub> gas on the block in a vacuum of  $\sim 10^{-5}$  Torr. Based on this result, an apparatus capable of implanting radioactivities to dry ice film was designed and installed at the beam line of KUR-ISOL (see Fig.1). This apparatus has two copper target blocks and one CO<sub>2</sub> gas diffuser in the vacuum chamber. Each copper target can be cooled with LN<sub>2</sub> flow internally and movable independently in a horizontal direction between the center of the chamber which is on the axis of the RI beam and the  $\gamma$ -ray measurement port while keeping LN<sub>2</sub> flow, and the surface temperatures are monitored with thermocouples. The diffuser is movable in a vertical direction and can be put in front of the left target, over which surface CO<sub>2</sub> gas is

sprayed uniformly. In the present work, about  $3 \times 10^6$  ions of  $^{146}\text{LaO}^+$  ( $T_{1/2} = 10$  s and 6 s) were implanted into dry ice film on the left target in every run. After the implantation, the right target was moved to the frontal vicinity of the left one and cooled down. Then the left target was warmed by stopping LN<sub>2</sub> flow after the right one was sufficiently cooled. With this procedure, it was examined whether released atoms of  $^{146}\text{Ce}$  ( $T_{1/2} = 14$  m, daughter of  $^{146}\text{La}$ ) and  $^{146}\text{Pr}$  ( $T_{1/2} = 24$  m, daughter of  $^{146}\text{Ce}$ ) from the left target were re-trapped on the right target together with CO<sub>2</sub>.

**RESULTS AND DISCUSSION:** From the measurements of the  $\gamma$ -rays emitted from both the targets, it was observed that a relatively large number of  $^{146}\text{Ce}$  and  $^{146}\text{Pr}$  were transferred from the left target to the right one when the dry ice film was sufficiently thick. Therefore, although the transfer efficiency is under analysis, this technique can be applied to the deuterium film method when recovering residual radioactivities in film safely.

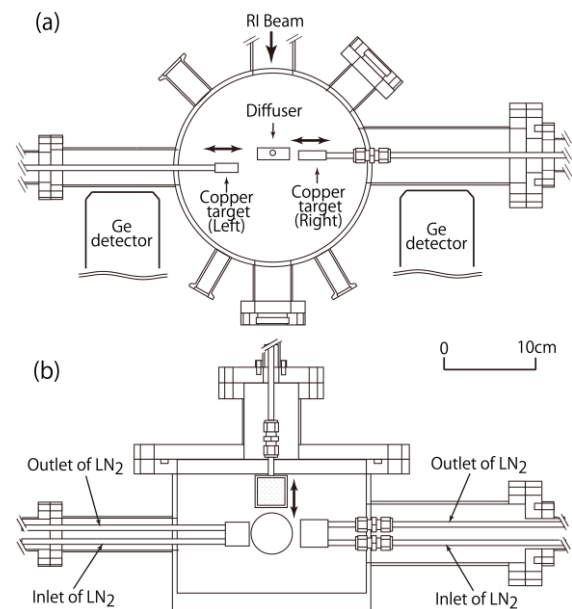


Fig.1. Main chamber for the RI beam implantation into dry ice film and for the transfer of the radioactivities. (a) Horizontal and (b) longitudinal section views.

**ACKNOWLEDGMENTS:** This research was partially supported by the Ministry of Education, Science, Sports and Culture, Grant-in-Aid for Scientific Research (C), 2012-2014 (24540303, Akihiro Taniguchi).

### REFERENCES:

- [1] G. Fricke *et al.*, At. Data Nucl. Data Tables **60** (1995) 177-285.
- [2] P. Strasser *et al.*, Hyperfine Interact. **193** (2009) 121-127.

## PR2-2 Identification of the Excited Levels of $^{156}\text{Pm}$ through the Decay of $^{156}\text{Nd}$

M. Shibata, R. Jyoushou<sup>1</sup>, Y. Shima<sup>1</sup>, K. Kosuga<sup>2</sup>,  
Y. Kojima, H. Hayashi<sup>3</sup> and A. Taniguchi<sup>4</sup>

Radioisotope Research Center, Nagoya University

<sup>1</sup>Graduate School of Engineering, Nagoya University

<sup>2</sup>School of Engineering, Nagoya University

<sup>3</sup>Institute of Health Biosciences, The University of Tokushima Graduate School

<sup>4</sup>Research Reactor Institute, Kyoto University

**INTRODUCTION:** Decay data of the fission products of  $^{235}\text{U}$  are important for nuclear engineering and also nuclear physics. In particular, doubly-odd nuclei are interesting in that their some of the excited states are interpreted as two-quasiparticle (2qp) ones. However, both experimental and theoretical studies of them far from the  $\beta$ -stability are scarce owing to their low yields.

The doubly-odd  $^{156}\text{Pm}$  was studied through the  $\beta$ -decay of  $^{156}\text{Nd}$  [1]. An isomeric state at 150.3 keV and two excited levels at 168.7 and 358.4 keV were proposed together with  $\gamma$ -rays having energies only up to 323 keV. On the basis of these results, the excited levels having the 2qp structure were theoretically constructed in the excitation energy ( $E_X$ ) up to 544 keV using the phenomenological rotor-particle model [2]. However, these studies focused only on the low  $E_X$  region. The  $Q_\beta$  value of  $^{156}\text{Nd}$  is 3690 keV [3]. Thus, excited levels are expected to be observed in a still higher  $E_X$  region. It is meaningful and interesting to propose a detailed level scheme for  $^{156}\text{Pm}$  and to confirm theoretical predictions experimentally.

In order to identify new excited levels of  $^{156}\text{Pm}$  and to determine the  $\gamma$ -ray intensities, the  $\beta$ -branching ratios and the  $\log-ft$  values, in the present work,  $\gamma$ -rays associated with the  $\beta$  decay of  $^{156}\text{Nd}$  were measured using a  $4\pi$  solid angle clover Ge detector [4].

**EXPERIMENTS:** The experiments were performed at the on-line mass separator KUR-ISOL at the Kyoto University Reactor, a 50 mg of 93%-enriched  $\text{UF}_4$  target being inserted in a through-hole.  $^{156}\text{Nd}$  isotopes were produced via the thermal neutron-induced fission of  $^{235}\text{U}$ . The  $^{156}\text{Nd}$  activities were transported by a gas jet of  $\text{He-N}_2$  mixed with a small amount of  $\text{O}_2$  and were ionized into  $\text{NdO}^+$  by a thermal-ionization type ion source. The mass-separated radioactive beam was incident on an aluminized Mylar tape set in the computer controlled tape transport system. The tape was moved every 10 s to reduce the background from their daughter nuclei.

$\gamma$ -rays associated with the decay of  $^{156}\text{Nd}$  were measured with a clover detector in the singles mode and the add-back mode. As described in [4], more intensive sum peaks of cascade  $\gamma$ -rays were observed in the add-back spectrum than in the singles one because the energies of cascade  $\gamma$ -rays are more effectively summed up with 4

Ge crystals, consequently observed peaks being expected to correspond to certain excited levels. An energy calibration of the detector was made in the range from 50 to 3500 keV using a standard  $\gamma$ -ray source  $^{152}\text{Eu}$  and a mass-separated fission product  $^{97}\text{Y}$ . The detector was shielded with 10-cm thick lead and borated polyethylene blocks to reduce the room background. A VME-based data acquisition system including a time stamp was used for a list mode.

**RESULTS:** The measured  $\gamma$ -ray spectra associated with the decay of  $^{156}\text{Nd}$  in the singles and add-back modes are shown in Fig. 1. The intensive peaks at 168.7 and 358.4 keV in [1] and the predicted excited levels, such as at 178.3, 220 and 274 keV in [2], were observed clearly in the add-back spectrum. It proves that a clover detector is useful for identifying excited levels. Other intensive peaks were observed in the energy region higher than 2000 keV. Some were ascribed to daughter nuclei of  $^{156}\text{Pm}$ , but the others, indicated with the closed circles in Fig. 1, are expected to newly excited levels in  $^{156}\text{Pm}$  from a preliminary analysis.

**CONCLUSIONS AND FUTURE PLAN:** New excited levels of  $^{156}\text{Pm}$  were identified along with new  $\gamma$ -rays associated with the decay of  $^{156}\text{Nd}$ . Hereafter, the energies of the excited levels will be deduced by analyzing  $\gamma$ - $\gamma$  coincidence relations and also the  $\gamma$ -ray intensities will be deduced from the singles spectrum by carrying out summing corrections according to the determined level structure.

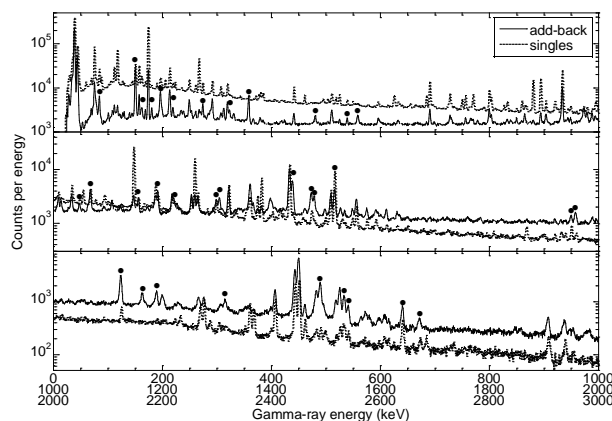


Fig. 1. The singles and add-back  $\gamma$ -rays spectra associated with the decay of  $^{156}\text{Nd}$ . The closed circles indicate excited levels of  $^{156}\text{Pm}$  that we considered to have been newly observed in the present work.

### REFERENCES:

- [1] M. Shibata *et al.*, *Eur. Phys. J. A* **31** (2007) 171-176.
- [2] P.C. Sood *et al.*, *Eur. Phys. J. A* **48** (2012) 136(1-6).
- [3] M. Wang *et al.*, *Chin. Phys. C* **36** (2012) 1603-2014.
- [4] Y. Shima *et al.*, *Appl. Rad. Isot.*, to be published.

採択課題番号 25P2-2 オンライン同位体分離装置と全吸収型検出器を用いた プロジェクト  
核分裂生成物の高エネルギー励起準位の解明

(名大・RIC) 柴田理尋、小島康明 (名大院・工) 嶋 洋佑、常少亮太 (名大・工) 小菅数人  
(徳島大・医) 林 裕晃 (京大・原子炉) 谷口秋洋

Y. Kojima, K. Kosuga<sup>1</sup>, Y. Shima<sup>2</sup>, R. Jyoushou<sup>1</sup>,  
H. Hayashi<sup>3</sup>, A. Taniguchi<sup>4</sup> and M. Shibata

Radioisotope Research Center, Nagoya University

<sup>1</sup>School of Engineering, Nagoya University

<sup>2</sup>Graduate School of Engineering, Nagoya University

<sup>3</sup>Institute of Health Biosciences, The University of Tokushima Graduate School

<sup>4</sup>Research Reactor Institute, Kyoto University

**INTRODUCTION:** Decay schemes are one of the most fundamental data about unstable nuclides. They are proposed from many measurements, and used in fields of nuclear applications such as nuclear energy engineering and nuclide identification, also in basic sciences to study nuclear structure.

In spite of many experimental efforts, only insufficient decay schemes are reported for many nuclides far from stability. This is due to experimental difficulties to produce these nuclides and their short half-lives. The fission product  $^{150}\text{Ce}$  is this example. The evaluated decay scheme of  $^{150}\text{Ce}$  includes only five excited levels and seven  $\gamma$ -rays [1]. Moreover, it is partially inconsistent with the decay scheme reported by Yamauchi *et al.* [2].

In order to resolve the discrepancy and to establish the reliable decay scheme, studies on  $^{150}\text{Ce}$  have been performed using the on-line isotope separator at KUR (KUR-ISOL). From  $\gamma$ -ray singles and  $\gamma$ - $\gamma$  coincidence measurements for mass-separated sources, a detailed decay scheme is proposed for  $^{150}\text{Ce}$ .

**EXPERIMENTS:** The  $^{150}\text{Ce}$  nuclides were produced by the thermal neutron induced fission of  $^{235}\text{U}$  at KUR-ISOL. The fission products were thermalized in the target chamber and transported to an ion source using a gas jet stream. After ionization, the Ce nuclides were extracted, accelerated, and mass-separated. The mass-separated nuclides were periodically moved to a detector port at time intervals of 12.2 s using a tape transport system.

$\gamma$ -ray singles and  $\gamma$ - $\gamma$  coincidence measurements were performed with two Ge detectors. Energy calibration of the detectors was made using standard  $\gamma$ -ray sources of  $^{241}\text{Am}$ ,  $^{133}\text{Ba}$  and  $^{152}\text{Eu}$ . Peak position shift during the measurements was monitored using intense  $\gamma$ -rays, and corrected in an off-line data analysis procedure. Detection efficiencies were also determined using standard sources. Coincidence summing effects were taken into account in deducing the full-energy peak efficiencies.

Signals from the detectors were processed by standard NIM modules. The data were accumulated in a list mode with a time stamp using a VME-based data acquisition system. About  $5 \times 10^7$  coincident events were collected in a measuring period of 46 h. To determine the half-life,  $\gamma$ -ray singles data were taken in a multi-spectrum mode

using eight 8192-channel pulse height analyzers, in which a 12-s counting time was divided into eight 1.5-s intervals.

**RESULTS:**  $\gamma$ -rays from the decay of  $^{150}\text{Pr}$  were observed in the spectrum together with those from  $^{150}\text{Ce}$ .  $\gamma$ -rays from the decay of  $^{150}\text{Ce}$  were mainly identified from coincidence relations with Pr KX-rays. A half-life of each  $\gamma$ -ray was also used for assigning its parent nuclide. For example, Fig. 1 shows decay curves of some intense  $\gamma$ -rays. From these curves, the half-life of 6.05(7) s was deduced for  $^{150}\text{Ce}$ , which approximately agrees with the value of 6.8(1) s in [2], but is obviously longer than the evaluated value of 4.0(6) s [1]. From the coincidence and half-life analysis, 58  $\gamma$ -rays were assigned to the decay of  $^{150}\text{Ce}$ .

Next, coincident spectra gated for all the  $\gamma$ -rays from  $^{150}\text{Ce}$  were analyzed in order to obtain  $\gamma$ - $\gamma$  coincidence relations. A decay scheme of  $^{150}\text{Ce}$  was established from these coincidence relations and  $\gamma$ -ray energy-sum relations. This decay scheme includes 18 excited levels and 54  $\gamma$ -rays. The  $\gamma$ -ray intensities were also deduced mainly from the singles spectrum. In the following, we only give comments on the 717-keV level because space is limited. The 717-keV level was reported in the evaluated data [1], but was not supported by our data; The 230-keV  $\gamma$ -ray, which was placed between the 717- and 488-keV level [1], was not coincident with the 180-, 279- and 378-keV  $\gamma$ -rays but with the 110- and 558-keV  $\gamma$ -rays. This results excluded the existence of the 717-keV level, and established a new level at 340 keV.

We are preparing a manuscript describing the decay scheme of  $^{150}\text{Ce}$  for publication.

**CONCLUSIONS AND FUTURE PLAN:** A detailed decay scheme including new 10 excited levels was constructed for  $^{150}\text{Ce}$ . We will deduce half-lives of excited levels in  $^{150}\text{Pr}$  on the basis of this decay scheme.

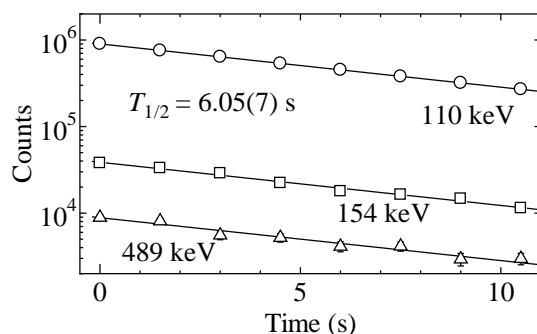


Fig.1. Decay curves of intense  $\gamma$ -rays from  $^{150}\text{Ce}$ .

#### REFERENCES:

- [1] S.K. Basu and A.A. Sonzogni, Nucl. Data Sheet **114** (2013) 435-660.
- [2] K. Yamauchi *et al.*, KURRI-KR-3 (1996), pp.51-53 (in Japanese).

W. Sato, R. Mizuuchi<sup>1</sup>, N. Irioka<sup>2</sup>, S. Komatsuda<sup>1</sup>, S. Kawata<sup>3</sup>, A. Taoka and Y. Ohkubo<sup>4</sup>

*Institute of Science and Engineering, Kanazawa University*

<sup>1</sup>*Graduate School of Natural Science and Technology, Kanazawa University*

<sup>2</sup>*School of Chemistry, Kanazawa University*

<sup>3</sup>*Department of Chemistry, Faculty of Science, Fukuoka University*

<sup>4</sup>*Research Reactor Institute, Kyoto University*

**INTRODUCTION:** Superionic conductivity observed for the silver iodide (AgI) has long been expected as an applicable property in a wide field of technology. This conducting phenomenon, however, emerges only at the high-temperature ( $\geq 420$  K)  $\alpha$  phase because of temperature-dependent crystal structures, which has been indeed a barrier to the practical applications of this compound.

Recently a novel technique overcame this situation: powder AgI coated with poly-N-vinyl-2-pyrrolidone (PVP) can drastically enhance the ionic transport property at room temperature, recording the conductivity of  $1.5 \times 10^{-2} \Omega^{-1} \text{cm}^{-1}$  [1]. The authors of [1] report that this achievement is due to successful control of the particle size as small as nanoscale. In addition to the property in the bulk, it is of great importance to obtain complementary information on the site-to-site hopping motion of  $\text{Ag}^+$  ions on an atomic scale for a detailed understanding of ionic conductivity of this binary solid. For that purpose, in the present work, dynamic behavior of  $\text{Ag}^+$  ions has been observed by means of the time-differential perturbed angular correlation (TDPAC) technique using the  $^{111}\text{Cd}(\leftarrow^{111}\text{Ag})$  probe nuclei. We here report successful observation of low temperature dynamic motion of  $\text{Ag}^+$  ions.

**EXPERIMENTS:** For the production of the TDPAC probe, Pd foil was irradiated with thermal neutrons in Kyoto University Reactor to produce  $^{111}\text{Pd}$ . After radioequilibrium was achieved between  $^{111}\text{Pd}$  and  $^{111}\text{Ag}$ , the Pd foil was dissolved in  $\text{HNO}_3$  aq. solution, and carrier-free  $^{111}\text{Ag}$  was isolated by an anion exchange chromatography. The separated  $^{111}\text{Ag}$  was incorporated together in PVP-coated AgI sample when the powder sample was synthesized by precipitation from the raw materials. We confirmed by transmission electron microscopy that microscopic particles with sizes of 10-100 nm were expectedly synthesized for  $^{111}\text{Ag}$ -free PVP-coated AgI.

TDPAC measurements of the  $^{111}\text{Cd}(\leftarrow^{111}\text{Ag})$  probe

were performed for the synthesized sample at various temperatures to observe temperature dependence of the spectra. The directional anisotropy,  $A_{22}G_{22}(t)$ , was deduced with the following relation:

$$A_{22}G_{22}(t) = 2 \frac{N(\pi, t) - N(\pi/2, t)}{N(\pi, t) + 2N(\pi/2, t)}. \quad (1)$$

Here,  $A_{22}$  denotes the angular correlation coefficient,  $G_{22}(t)$  the time-differential perturbation factor as a function of the time interval,  $t$ , between the relevant cascade  $\gamma$ -ray emissions, and  $N(\theta, t)$  the number of the delayed coincidence events observed at an angle,  $\theta$ .

**RESULTS:** Fig. 1 shows the TDPAC spectra of the  $^{111}\text{Cd}(\leftarrow^{111}\text{Ag})$  probe introduced in PVP-coated AgI measured at different temperatures. The exponential relaxation of the directional anisotropy seen in Fig. 1(a) undoubtedly signifies that the probe is dynamically perturbed by the extranuclear field. This phenomenon is understandable because the measurement was done in the temperature range at which the  $\alpha$  phase is stabilized. What is to be noted here is that the spectral relaxation was also observed even at the temperature as low as 333 K as shown in Fig. 1(b). It was found from this observation that  $\text{Ag}^+$  ions surrounding the probe nuclei exhibit site-to-site hopping motion in the present PVP-coated AgI nanoparticle; this would be the first atomic-level observation of  $\text{Ag}^+$  hopping. Further investigation on temperature dependence of the relaxation rates would lead to determination of the activation energy of the local motion.

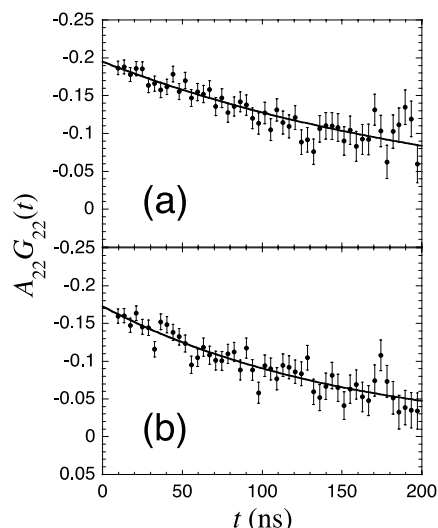


Fig. 1. TDPAC spectra of  $^{111}\text{Cd}(\leftarrow^{111}\text{Ag})$  in PVP-coated AgI (a) at 453 K and (b) at 333 K.

#### REFERENCE:

[1] R. Makiura *et al.* *Nature Mater.* **8** (2009) 476-480.

M. Tsuneyama, M. Tanigaki<sup>1</sup>, A. Taniguchi<sup>1</sup>, Q. Xu<sup>1</sup> and Y. Ohkubo<sup>1</sup>

Graduate School of Science, Kyoto University  
<sup>1</sup>Research Reactor Institute, Kyoto University

**INTRODUCTION:** Magnetic hyperfine fields  $B_{\text{HFF}}$  in materials are useful in testing first-principle calculations in condensed matter physics. Although for typical- and transition-element impurities in Fe, theoretical  $B_{\text{HFF}}$  values are in good agreement with those of experiments, this is not the case for lanthanide impurities in Fe. Moreover, there are few reliable experimental  $B_{\text{HFF}}$  values available.

In the case of Pm impurities in Fe, two experimental results of  $B_{\text{HFF}}$  are reported:  $B_{\text{HFF}} = 406 \pm 100$  T [1] and  $284 \pm 35$  T [2]. These experiments were performed by low-temperature nuclear orientation method. However, these values are not reliable because a two-site model was used in both data analyses that assumes only two sites as the sites of the impurities, having either full or no  $B_{\text{HFF}}$ . In order to obtain a reliable  $B_{\text{HFF}}$  at Pm impurities in Fe, in this work we attempted to employ the time-differential perturbed-angular-correlation (TDPAC) method.

**EXPERIMENTS:** The sample was prepared by the ion implantation technique with KUR-ISOL [3].  $^{147}\text{Nd}$  decaying to  $^{147}\text{Pm}$  were mass-separated from the fission products of thermal-neutron-irradiated  $^{235}\text{U}$  and implanted in an Fe foil after accelerated to 100 keV with the post accelerator. The number of  $^{147}\text{Nd}$  ( $I^\pi = 5/2^-$ ,  $T_{1/2} = 10.98$  d) in the foil was about  $7.4 \times 10^4$ .

TDPAC measurements were performed in the following two geometries:

- 3 counters: The correlation angles were  $\theta = \pm 135^\circ$  and three BaF<sub>2</sub> scintillation counters were used. A 0.3-T magnetic field was applied to the sample perpendicular to the detector plane.
- 4 counters: The correlation angles were  $\theta = 90^\circ, 180^\circ$  and four BaF<sub>2</sub> detectors were used. A 0.8-T magnetic field was applied to the sample perpendicular to the detector plane.

Spin precession of the 91 keV state in  $^{147}\text{Pm}$  ( $I^\pi = 5/2^+$ ,  $\mu = 3.22 \pm 0.16 \mu_N$ ,  $T_{1/2} = 2.50$  ns) was observed through the 440–91 keV  $\gamma$ -cascade. The Larmor frequency  $\omega_L$  and the angular correlation coefficient  $A_{22}$  were determined with the least-squares method.

**RESULTS:** The TDPAC spectra and the results of the least-squares fits are shown in Fig. 1 and Table 1, respectively. In this experiment, we were not successful in obtaining the value of  $B_{\text{HFF}}$  at Pm impurities in Fe because of the very large statistical errors. As seen in Table 1, the

statistical errors of the  $A_{22}$  values are both larger than 100%. Since the  $A_{22}$  is consistent with 0, the  $\omega_L$  is undefined. To solve the problem, it is necessary to increase considerably the number of implanted  $^{147}\text{Nd}$ .

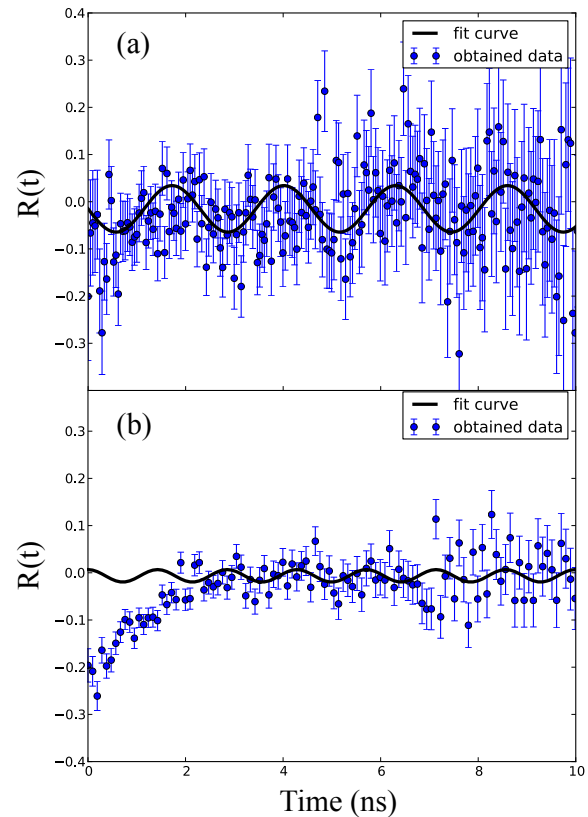


Fig. 1. Results of the TDPAC measurements with (a)  $\theta = \pm 135^\circ$  and (b)  $\theta = 90^\circ, 180^\circ$  correlations. The dots and the lines represent the data and the fit results, respectively.

Table 1. Results obtained with the least-squares fit. The expected  $\omega_L$  value was deduced simply assuming  $B_{\text{HFF}} = 100$  T. The units of  $\omega_L$  is Grad/s.

	calculation	3 counters	4 counters
$A_{22}$	0.0525	$0.589 \pm 1.141$	$0.011 \pm 0.250$
	expected value	3 counters	4 counters
$\omega_L$	$ 6.17 $	$-1.37 \pm 0.13$	$ 2.20 \pm 1.75 $

#### REFERENCES:

- [1] B.D.D. Singleton *et al*, *Hyp. Interact.* **75** (1992) 471.
- [2] J. Goto *et al*, *Hyp. Interact.* **136/137** (2001) 561.
- [3] A. Taniguchi, M. Tanigaki and Y. Ohkubo, *Nucl. Instr. Meth.* **B 317** (2013) 476.

S. Komatsuda, W. Sato<sup>1</sup> and Y. Ohkubo<sup>2</sup>

Graduate School of Natural Science and Technology,  
Kanazawa University

<sup>1</sup>Institute of Science and Engineering, Kanazawa University

<sup>2</sup>Research Reactor Institute, Kyoto University

**INTRODUCTION:** Impurity-induced properties emerging in ZnO has been attracting increasing attention toward its application to functional materials in a wide field of industry. For a practical use of ZnO as a conduction-controlling device, it is of great importance to study the physical and chemical states of doped impurities and/or oxygen vacancies. From this point of view, we have investigated the factors determining the local structures and their stability for the Al-doped ZnO samples synthesized on different conditions by means of the time-differential perturbed angular correlation (TDPAC) method. In a series of our TDPAC studies, drastic change of the local structure was observed for Al-doped ZnO sample heat-treated in vacuum [1]. In order to provide insight into the effect of the heat-treatment condition, in the present work, we examined the structural change for Al-doped ZnO prepared by long heating in vacuum.

**EXPERIMENTS:** For the synthesis of 100 ppm Al-doped ZnO, stoichiometric amounts of  $\text{Al}(\text{NO}_3)_3 \cdot 9\text{H}_2\text{O}$  and ZnO powder were mixed in ethanol. The suspension was heated to evaporate the ethanol until dryness. The powder was pressed into two disks and sintered in air at 1273 K for 3 h. After that, the disks were separately ground into powder and sealed in quartz tubes in vacuum, respectively. They underwent further heat treatment in vacuum at 1273 K for 100 h. About 3 mg of CdO enriched with  $^{110}\text{Cd}$  was irradiated with thermal neutrons in a pneumatic tube at Kyoto University Reactor, and radioactive  $^{111\text{m}}\text{Cd}$  was generated by  $^{110}\text{Cd}(n, \gamma)^{111\text{m}}\text{Cd}$  reaction. The neutron-irradiated CdO powder was then separately added into the disks and mixed again in a mortar for 20 min. Each of the mixtures was pressed into disks. The samples were sintered in different atmosphere: one was in air and the other in vacuum at 1373 K for 45 min. TDPAC measurements were carried out for the  $^{111}\text{Cd}(\leftarrow^{111\text{m}}\text{Cd})$  probe on the 151–245 keV cascade  $\gamma$  rays with the intermediate state of  $I = 5/2$  having a half-life of 85.0 ns.

**RESULTS:** Fig. 1 shows the TDPAC spectra of  $^{111}\text{Cd}(\leftarrow^{111\text{m}}\text{Cd})$  probe in 100 ppm Al-doped ZnO annealed (a) in air and (b) in vacuum. The directional anisotropy on the ordinate,  $A_{22}G_{22}(t)$ , was deduced by the following relation for delayed coincidence events of the cascade:

$$A_{22}G_{22}(t) = \frac{2[N(\pi, t) - N(\pi/2, t)]}{N(\pi, t) + 2N(\pi/2, t)}$$

Here,  $A_{22}$  denotes the angular correlation coefficient,  $G_{22}(t)$  the time-differential perturbation factor as a function of the time interval,  $t$ , between the relevant cascade  $\gamma$ -ray emissions, and  $N(\theta, t)$  the number of the coincidence events observed at angle,  $\theta$ . The value of the electric field gradient at the probe nucleus is  $1.7(3) \times 10^{21} \text{ Vm}^{-2}$  for both spectra in Fig. 1(a) and 1(b), which suggests that the  $^{111}\text{Cd}(\leftarrow^{111\text{m}}\text{Cd})$  probe resides at the substitutional Zn site regardless of the presence of Al impurities in the system [2]. With respect to Fig. 1(b), the spectral damping appears as a result of large distribution of the quadrupole frequency  $\delta (= 8.9(6)\%)$ . It is generally known that oxygen vacancies are likely formed in high-temperature vacuum in oxide compounds. In view of this, the large  $\delta$  value could be attributed to formation of oxygen vacancies around the probe during annealing process in vacuum. For further information on the state of impurities and/or oxygen vacancies, the annealing-time and annealing-temperature dependences of this local structure need to be investigated.

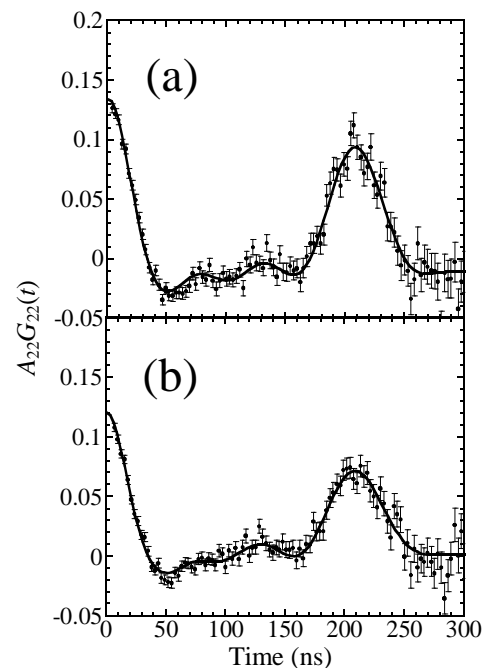


Fig. 1. TDPAC spectra of  $^{111}\text{Cd}(\leftarrow^{111\text{m}}\text{Cd})$  in 100 ppm Al-doped ZnO annealed (a) in air and (b) in vacuum.

#### REFERENCES:

- [1] S. Komatsuda, W. Sato and Y. Ohkubo, *J. Radioanal. Nucl. Chem.* Accepted for publication.  
[2] S. Komatsuda, W. Sato, S. Kawata and Y. Ohkubo, *J. Phys. Soc. Jpn.* **80** (2011) 095001.



Y. Kobayashi, S. Kitao, M. Kurokuzu, Y. Negishi<sup>1</sup>,  
T. Tsukuda<sup>2</sup>, N. Kojima<sup>3</sup> and M. Seto

Research Reactor Institute, Kyoto University

<sup>1</sup>Department of Applied Chemistry, Tokyo University of Science

<sup>2</sup>Department of Chemistry, The University of Tokyo

<sup>3</sup>Graduate School of Arts and Sciences, The University of Tokyo

## Introduction

Metallic nanoparticles are interesting in their peculiar properties. Previously, we performed a <sup>197</sup>Au Mössbauer study on Au<sub>25</sub>(SG)<sub>18</sub> (SG: glutathione) and obtained the result that the area ratio and the parameters of the Mössbauer spectrum were quite consistent with the structure elucidated from an X-ray diffraction study on its single crystal [1]. In this work, we performed a Mössbauer study using Au nanoparticles of different sizes to elucidate the structures of nanoparticles.

## Experimental Procedure

Nanoparticles Au<sub>25</sub>(SC<sub>12</sub>H<sub>25</sub>)<sub>18</sub> and Au<sub>38</sub>(SC<sub>12</sub>H<sub>25</sub>)<sub>24</sub> were prepared by reduction of Au ions and refined by electrophoreses [2]. The SC<sub>12</sub>H<sub>25</sub>, 1-dodecanethiol, works as a surfactant to hinder the fusion of nanoparticles. In the <sup>197</sup>Au Mössbauer measurements, the  $\gamma$ -ray source was <sup>197</sup>Pt in Pt foil, which was prepared by the <sup>196</sup>Pt(n,  $\gamma$ )<sup>197</sup>Pt reaction using KUR. The spectroscopy measurements were performed at 13 K. In the spectra, zero-velocity positions were defined as the peak position for pure Au.

## Results and Discussion

Fig. 1 shows the <sup>197</sup>Au Mössbauer spectra of Au<sub>25</sub>(SC<sub>12</sub>H<sub>25</sub>)<sub>18</sub> and Au<sub>38</sub>(SC<sub>12</sub>H<sub>25</sub>)<sub>24</sub> nanoparticles. Each spectrum is composed of 3 subspectra. Subspectrum 1 showing a large quadruple splitting is due to the Au atoms making a chain with the S atom of dodecanethiol on the surface of the nanoparticle. Subspectrum 3 shows zero quadruple splitting and thus this comes from the Au atom at the center of the particles. Subspectrum 2 showing a rather small quadruple splitting is due to the Au atoms covering the center Au atom.

The area ratio of these subspectra for Au<sub>25</sub>(SC<sub>12</sub>H<sub>25</sub>)<sub>18</sub> is 46, 42 and 10%. In the reported structure of the Au<sub>25</sub> nanoparticle, the numbers of the Au atoms for the three components are 12, 12 and 1, so the ratio of the Au atoms is 48, 48 and 4%. These two sets of values almost agree, but the value for subspectrum 3, 10%, is larger than the corresponding value of 4%. This discrepancy is considered to arise from the recoilless fraction of spectrum 3, which comes from the center of the Au core, being bigger than those for the other two components.

The area ratio of the three subspectra for Au<sub>38</sub>(SC<sub>12</sub>H<sub>25</sub>)<sub>24</sub> is 30, 55 and 15%, which is not so different from that for Au<sub>25</sub>(SC<sub>12</sub>H<sub>25</sub>)<sub>18</sub>. According to the structure of the Au<sub>38</sub> nanoparticle suggested from an

X-ray diffraction study [3], the numbers of the Au atoms of the three components are 15, 21 and 2. The ratio of the Au atoms is therefore 39, 55 and 5%. This number ratio does not agree with the corresponding area ratio in the Mössbauer spectrum, the area ratio of subspectrum 1, 30%, being smaller than the Au atom ratio, 39%. The Au<sub>38</sub> nanoparticle has a bigger core (components 2 and 3) than Au<sub>25</sub>, so the recoilless fractions of these components are large. This result shows that the relation between the area ratio of the subspectra and the numbers of the Au atoms is not unique. We need more study to elucidate the structure of nanoparticles using Mössbauer spectroscopy.

## Conclusion

The <sup>197</sup>Au Mössbauer spectrum for the Au<sub>38</sub>(SC<sub>12</sub>H<sub>25</sub>)<sub>24</sub> nanoparticle consists mainly of three components, which is the same for the Au<sub>25</sub>(SC<sub>12</sub>H<sub>25</sub>)<sub>18</sub> nanoparticle. However, the recoilless fractions of the components are different, so the relation between the area ratio of the subspectra and the numbers of the Au atoms is not unique.

## References

- [1] K. Ikeda, Y. Kobayashi, Y. Negishi, M. Seto, T. Iwasa, K. Nobusada, T. Tsukuda and N. Kojima, *J. Am. Chem. Soc.* **129** (2007) 7230.
- [2] Y. Negishi, K. Nobusada and T. Tsukuda, *J. Am. Chem. Soc.* **127** (2005) 5261.
- [3] H. Qian, W. T. Eckenhoff, Y. Zhu, T. Pintauer and R. Jin, *J. Am. Chem. Soc.* **132** (2010) 8280.

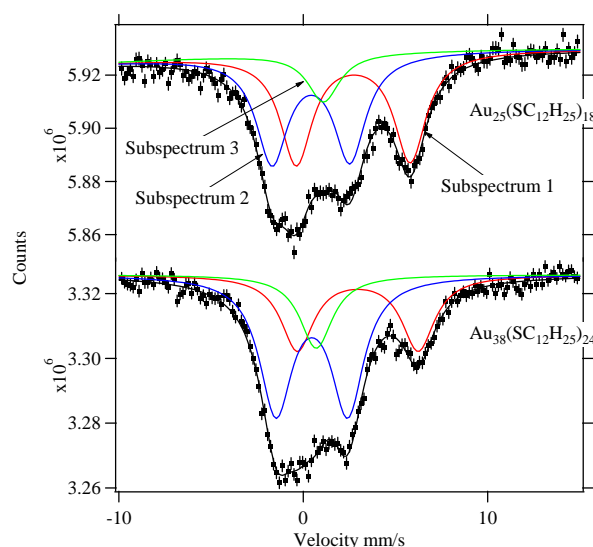


Fig. 1. <sup>197</sup>Au Mössbauer spectra for Au<sub>25</sub>(SG)<sub>18</sub> and Au<sub>38</sub>(SC<sub>12</sub>H<sub>25</sub>)<sub>24</sub> nanoparticles.

## PR2-8 Determination of the Structure and Electronic State of Thiolate-Protected Hetero-Metal Cluster, $\text{Au}_{24}\text{Pd}_1(\text{SC}_{12}\text{H}_{25})_{18}$ , by Means of $^{197}\text{Au}$ Mössbauer Spectroscopy

N. Kojima, Y. Kobayashi<sup>1</sup> and M. Seto<sup>1</sup>

Graduate School of Arts and Sciences, The University of Tokyo

<sup>1</sup>Research Reactor Institute, Kyoto University

**INTRODUCTION:** In the last decade, small gold clusters composed of less than 100 atoms protected by organic ligands have attracted much attention as a prototypical system for fundamental studies on quantum size and as a building block of nano-scale devices [1]. Among small gold clusters, the thiolate-protected gold cluster,  $\text{Au}_{25}(\text{SR})_{18}$ , has been studied most extensively as a prototype system of stable  $\text{Au}_n(\text{SR})_m$  clusters [2]. According to the structural analysis,  $\text{Au}_{25}(\text{SC}_2\text{H}_4\text{Ph})_{18}$  is composed of an icosahedral  $\text{Au}_{13}$  core whose surface is protected by six staples,  $-\text{S}(\text{R})-\text{Au}-\text{S}(\text{R})-$  [3]. Based on the geometrical structure of  $\text{Au}_{25}(\text{SC}_2\text{H}_4\text{Ph})_{18}$ , we have successfully analyzed the  $^{197}\text{Au}$  Mössbauer spectra of glutathionate-protected gold clusters,  $\text{Au}_n(\text{SG})_m$  with  $n = 10 - \sim 55$  [4]. The aim of the present project is to investigate the structure and the electronic state of thiolate-protected hetero-metal cluster,  $\text{Au}_{24}\text{Pd}_1(\text{SC}_{12}\text{H}_{25})_{18}$ , by means of  $^{197}\text{Au}$  Mössbauer spectroscopy.

**EXPERIMENTS:**  $^{197}\text{Au}$  Mössbauer spectra were recorded at the Research Reactor Institute of Kyoto University.  $^{197}\text{Pt}$  was generated as the  $\gamma$ -ray source (77.3 keV) by irradiating a 98%-enriched  $^{196}\text{Pt}$  metal foil with neutrons. The temperatures of the  $\gamma$ -ray source and samples were kept at 16 K. Mössbauer parameters, isomer shift (*IS*) and quadrupole splitting (*QS*), were determined by fitting the spectra using MossWinn 3.0 program [5]. The spectra were calibrated and referenced by using the six lines of a body-centered cubic iron foil ( $\alpha$ -Fe). The *IS* of Au foil was referenced to 0 mm/s.

**RESULTS:** The  $^{197}\text{Au}$  Mössbauer spectra of  $\text{Au}_{25}(\text{SC}_{12}\text{H}_{25})_{18}$  and  $\text{Au}_{24}\text{Pd}_1(\text{SC}_{12}\text{H}_{25})_{18}$  are shown in Fig. 1 [6]. These spectra were analyzed based on the structure of  $\text{Au}_{25}(\text{SR})_{18}$  ( $\text{SR} = \text{SC}_2\text{H}_4\text{Ph}$ ). The line profile of  $^{197}\text{Au}$  Mössbauer spectra for  $\text{Au}_{25}(\text{SC}_{12}\text{H}_{25})_{18}$  can be reproduced well by the superposition of a singlet corresponding to the Au3 site and two doublets corresponding to the Au1 and Au2 sites (Fig. 2(a)) [6]. The analysis of  $\text{Au}_{25}(\text{SC}_{12}\text{H}_{25})_{18}$  gave the following Mössbauer parameters: *IS* = 2.71 mm/s and *QS* = 6.71 mm/s for Au1; *IS* = 0.41 mm/s and *QS* = 4.22 mm/s for Au2; and *IS* = 1.10 mm/s and *QS* = 0.00 mm/s for Au3 [6]. The Mössbauer parameters for Au1 are similar to those of Au(I) coordinated by two sulfur atoms [7].

The occupation site of the Pd dopant within  $\text{Au}_{24}\text{Pd}_1(\text{SC}_2\text{H}_4\text{Ph})_{18}$  was determined by the  $^{197}\text{Au}$  Mössbauer spectroscopy. The contribution from the central Au atom observed in the monometallic  $\text{Au}_{25}(\text{SC}_{12}\text{H}_{25})_{18}$  counterpart obviously disappeared in the  $^{197}\text{Au}$  Mössbauer spectrum of  $\text{Au}_{24}\text{Pd}_1(\text{SC}_{12}\text{H}_{25})_{18}$  (Fig. 1(b)). Therefore, we concluded that the single Pd atom doped in  $\text{Au}_{24}\text{Pd}_1(\text{SC}_2\text{H}_4\text{Ph})_{18}$  is located at the center of the icosahedral  $\text{Au}_{12}\text{Pd}$  core.

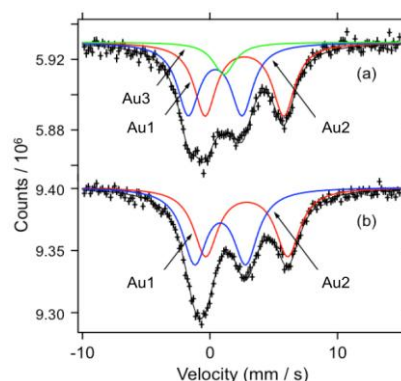


Fig. 1.  $^{197}\text{Au}$  Mössbauer spectra of (a)  $\text{Au}_{25}(\text{SC}_{12}\text{H}_{25})_{18}$  and (b)  $\text{Au}_{24}\text{Pd}_1(\text{SC}_{12}\text{H}_{25})_{18}$  [6]. The Au1, Au2, and Au3 spectra correspond to the Au atoms in the  $-\text{S}(\text{R})-\text{Au}-$  oligomers, at the surface of the Au core, and within the Au core, respectively.

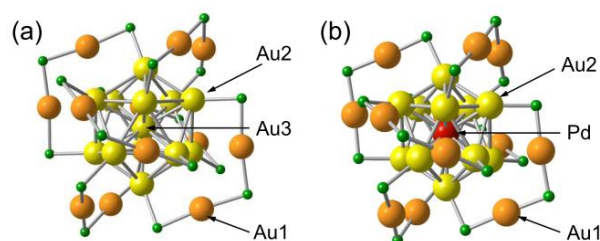


Fig. 2. Structural framework of (a)  $\text{Au}_{24}\text{Pd}(\text{SR})_{18}$  and (b)  $\text{Au}_{24}\text{Pd}(\text{SR})_{18}$  [6]. Large and small balls represent Au and S atoms, respectively. The R group is omitted for simplicity.

### REFERENCES:

- [1] M.-C. Daniel, D. Astruc, *Chem. Rev.* **104** (2004) 293.
- [2] (a) T. G. Schaff, R. L. Whetten, *J. Phys. Chem. B* **104** (2009) 2630, (b) R. C. Price, R. L. Whetten, *J. Am. Chem. Soc.* **127** (2005) 13750, (c) H. Tsunoyama, Y. Negishi, T. Tsukuda, *J. Am. Chem. Soc.* **128** (2006) 6036.
- [3] (a) M. W. Heaven, A. Dass, P. S. White, K. M. Holt, R. W. Murray, *J. Am. Chem. Soc.* **130** (2008) 3754, (b) M. Zhu, E. Lanni, N. Garg, M. E. Bier, R. Jin, *J. Am. Chem. Soc.* **130** (2008) 1138.
- [4] N. Kojima, Y. Kobayashi, Y. Negishi, M. Seto, T. Tsukuda, *Hyperfine Interactions* **217** (2013) 91.
- [5] MossWinn – Mössbauer spectrum analysis and database software. <http://www.mosswinn.com/>.
- [6] Y. Negishi, W. Kurashige, Y. Kobayashi, S. Yamazoe, N. Kojima, M. Seto, T. Tsukuda, *J. Phys. Chem. Lett.* **4** (2013) 3579.
- [7] *Mössbauer Handbooks:  $^{197}\text{Au}$  Mössbauer spectroscopy*, Mössbauer Effect Data Center, The University of North Carolina, U.S.A. (1993).

## PR2-9 Characterization of Au in Nickel Oxide by $^{197}\text{Au}$ Mössbauer Spectroscopy

T. Yokoyama, H. Ohashi<sup>1</sup>, Y. Kobayashi<sup>2</sup>, Y. Okaue, D. Kawamoto, H. Ando and S. Kitao<sup>2</sup>

Faculty of Sciences, Kyushu University

<sup>1</sup> Faculty of Arts and Science, Kyushu University

<sup>2</sup> Research Reactor Institute, Kyoto University

**INTRODUCTION:** Gold nanoparticles supported on nickel oxide have been used as various oxidation-reduction catalysts [1]. It is essential to characterize them for understanding their advantages and establishing the guideline for their syntheses with high activity. For the characterization of supported gold catalysts, their oxidation states have been determined by X-ray absorption spectroscopy (XAS) and their crystal phases have been detected by powder X-ray diffraction (XRD). However, supported gold catalysts have rarely been characterized by  $^{197}\text{Au}$  Mössbauer spectroscopy because of technical difficulties.

In this study, the detailed chemical states of gold supported on nickel oxide catalysts were investigated using  $^{197}\text{Au}$  Mössbauer spectroscopy and results of X-ray absorption near edge structure (XANES) with which technique the oxidation states and structures for various metals can be observed.

**EXPERIMENTS:** Precursors of supported gold catalysts ( $\text{Au}/\text{NiO}_x$ ) were prepared by the coprecipitation method. Aqueous mixed solutions of  $\text{HAuCl}_4$  and  $\text{Ni}(\text{NO}_3)_2$  with three Au/Ni ratios (1:19, 1:30 and 1:40) were poured into NaOH solutions under stirring. The precipitates were filtered, washed and freeze-dried. The obtained powders were precursors of supported gold catalysts.

The chemical states of gold in the solid samples (precursors) obtained were determined by  $^{197}\text{Au}$  Mössbauer spectroscopy (home-made equipment).  $^{197}\text{Pt}$  isotopes ( $T_{1/2} = 18.3$  h), a  $\gamma$ -ray source feeding the 77.3-keV Mössbauer transition of  $^{197}\text{Au}$ , were prepared by neutron irradiation of isotopically enriched  $^{196}\text{Pt}$  metal at the Kyoto University Reactor. The absorbers were the particle specimens. The source and the specimens were cooled with a helium refrigerator. The temperatures of the specimens were in the range 8–15 K. The zero velocity point of the spectra was the peak point of pure bulk gold. The spectra for all the solid samples were fitted with Lorentzian functions.

Furthermore, for these catalysts, the Ni K-edge and  $\text{AuL}_3$ -edge XANES were measured at BL14B2 of SPring-8 (Hyogo, Japan).

**RESULTS:** The Ni K-edge XANES spectra for all the precursors of  $\text{Au}/\text{NiO}_x$  catalysts revealed that the chemical states of nickel were  $\text{Ni}(\text{OH})_2$ . The Au  $\text{L}_3$ -edge XANES spectra for the precursors confirmed the pres-

ence of Au(0) and Au(III). Fig. 1 shows the  $^{197}\text{Au}$  Mössbauer spectra for the precursors and standard materials. From the  $^{197}\text{Au}$  Mössbauer spectra, Au(0) and Au(III) were also seen in the precursors. Even with no specific reducing reagent, Au(III) in the precursors were unexpectedly reduced to Au(0). This unique reduction mechanism will be elucidated in near future.

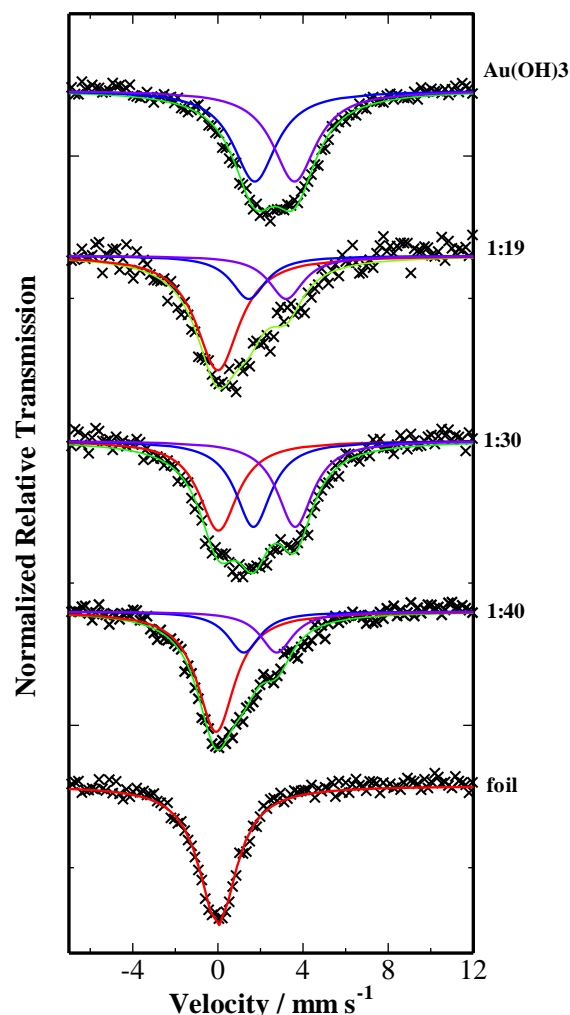


Fig. 1.  $^{197}\text{Au}$  Mössbauer spectra for the precursors of  $\text{Au}/\text{NiO}_x$  catalysts and for two standard materials,  $\text{Au}(\text{OH})_3$  and Au foil. The ratios at the right side represent the Au/Ni ratios.

### REFERENCE:

[1] H. Nishikawa *et al.*, *Adv. X-Ray Chem. Anal. Jpn.* **43** (2012) 285-292 (in Japanese).